Top Catal (2010) 53:40–48
DOI 10.1007/s11244-009-9437-4

ORIGINAL PAPER

Catalyst Structure-Performance Relationship Identified by High-Throughput *Operando* Method: New Insight for Silica-Supported Vanadium Oxide for Methanol Oxidation

Guosheng Li · Dehong Hu · Guanguang Xia · Z. Conrad Zhang

Published online: 22 December 2009
© Springer Science+Business Media, LLC 2009

Abstract The reaction mechanism of methanol oxidation catalyzed by vanadium oxides on a silica support (V_2O_5/SiO_2) was investigated in a high-throughput *operando* reactor coupled with a Fourier transform-infrared (FT-IR) imaging system for rapid product analysis and six parallel, in situ Raman spectroscopy probes for catalyst characterization. Up to six V_2O_5/SiO_2 catalysts with different vanadium loadings (i.e., from 0 to 7%) were simultaneously monitored under identical experimental conditions. The specific Raman bands of the different catalysts in the six parallel reaction channels are quantitatively determined in this work. Under steady-state reaction conditions, the Raman intensities of C–H stretch in Si–O–CH_3 and V–O–CH_3 were extensively studied at different reaction temperatures and different vanadium loadings. *For the first time*, we observed enhanced Si–O–CH_3 formation on V_2O_5/SiO_2 catalysts with low vanadium loadings. We attribute this phenomenon to *surface cluster edge activation*. Careful comparison of the in situ Raman intensity of V–O–CH_3 on V_2O_5/SiO_2 catalysts revealed different methoxy formation mechanisms in different reaction temperature regimes.

Keywords FT-IR imaging · In situ Raman spectroscopy · High throughput reactor · Methoxy group · Vanadium catalysts · Metal oxide catalysts · Methanol oxidation · Surface cluster-edge activation

G. Li · D. Hu · G. Xia · Z. C. Zhang
Institute for Interfacial Catalysis, Pacific Northwest National Laboratory, Richland, Washington 99352, USA

Z. C. Zhang (✉)
KiOR Inc., 13001 Bay Park Road, Pasadena, TX 77507, USA
e-mail: conrad.zhang@kior.com

1 Introduction

Understanding correlations between active surface structures of heterogeneous catalysts and their catalytic performance is important for fundamental research in catalysis and for catalyst developments in industry [1, 2]. Active surface structures of heterogeneous catalysts are often dynamic and are very sensitive to the reaction environment; therefore, it is particularly desirable to study the active sites under *operando* conditions [3].

Supported V_2O_5 catalysts play an important role for a number of industrially important reactions including selective oxidation of *o*-xylene to phthalic anhydride [4], selective catalytic reduction of NO_x [5], and methanol partial oxidation reaction [6–8]. Many studies that focused on understanding correlations between the surface structure of vanadium oxide, the supporting material, and their catalytic performance have been reported in the literature [9–12]. To better understand the reaction mechanism, it is important to be able to interrogate, at a molecular level, the structure of a supported vanadium oxide catalyst and intermediates formed during the reaction. Various types of spectroscopic techniques, including Raman spectroscopy [13–17], extended X-ray absorption fine structure (EXAFS) [18, 19], IR [20, 21], solid-state ^{51}V nuclear magnetic resonance (NMR) [22], etc., have been used to investigate structural information for the monolayer and sub-monolayer surface coverage of vanadium oxide catalysts on different oxide supports.

The most widely accepted molecular structure (pyramidal model) for vanadium oxide support assumes that vanadium oxide is present as an isolated VO_4 unit consisting of a terminal V = O bond perpendicular to the surface and three bridging V–$O_{support}$ bonds [23, 24]. The bond length of the V = O has been estimated in the range

1.60–1.79 Å (depending on the support material) based on measured Raman frequencies and using empirical correlations [25]. The following vanadium–oxygen bond lengths for a pyramidal model were obtained from functional theory (DFT) simulations: 1.59 Å for the V = O terminal bond and 1.83 Å for the three V–O bond (i.e., the $V–O_{support}$ bridging bonds) [26]. For V_2O_5 oligomers, V–O–V bridging bonds were expected to form by linking the VO_4 units in the pyramidal model [27, 28].

In a postulated reaction mechanism for methanol partial oxidation on V_2O_5/SiO_2 catalysts [10], the first step is methoxy formation on VO_4 units by breaking one of the three V–O–Si bonds. The selectivity toward formaldehyde (FA) implies the desorption of FA from $V–O=CH_2$, which is produced from the oxidation of $V–OCH_3$ before further oxidation to dioximethylene. A detailed mechanism of this dehydrogenation process has not been fully determined yet, although a V = O bond has been proposed to be involved in this C–H bond cleavage [29].

In our study, we applied a home-built, high-throughput *operando* (HTO) reactor to partially oxidize methanol on V_2O_5/SiO_2 catalysts. In this prototype HTO reactor, six in situ Raman probes simultaneously collected Raman scattering signals from six catalysts in parallel reaction channels, and a FT-IR imaging system was used to analyze reaction products of all reaction channels simultaneously. By integrating in situ Raman spectroscopy and FT-IR imaging technique in this HTO reactor, new insights were gained on the mechanism of methoxy formation on V_2O_5/SiO_2 catalysts. The results from this study are crucial in establishing a relationship between catalytic activity and dynamic structures of catalysts.

2 Experimental

2.1 FT-IR Imaging System

As shown in Fig. 1, our FT-IR imaging system consists of a Bruker Vertex 70 FT-IR spectrometer, our HTO reactor, a focal plane array (FPA) detector, two gold-coated mirrors, and a lens assembly. Our HTO reactor, which has been described in detail elsewhere [30], is briefly described below. The FT-IR spectrometer provides a modulated infrared beam with a diameter of ~40 mm from its outlet port. The infrared beam shown as white arrows in Fig. 1 passes through the HTO reactor, which has six parallel reaction channels. The beam then is refocused onto the FPA detector using a lens assembly, which consists of two lenses embedded in a long optical tube (~1 m) to ensure a good optical alignment. The combination of two ZnSe lenses provides a magnification ratio (typically 0.1) that can be adjusted easily by changing the distance of the two

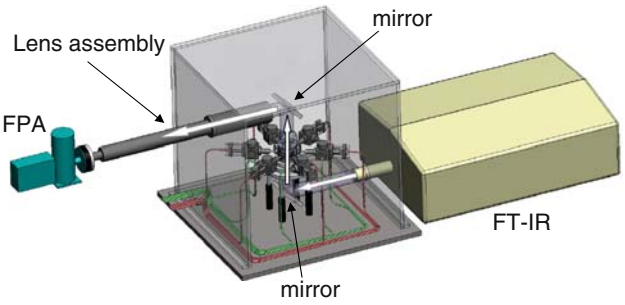

Fig. 1 Schematic diagram of the experimental setup

lenses. By using the lens assembly, the image of the six reaction channels (~40 mm) was fully captured on the FPA detector (chip size of 5 mm) in our experiment. The entire IR beam pass, which includes the FT-IR spectrometer, the HTO reactor in an acrylic box, and the lens assembly, were purged with pure N_2 gas to avoid any spectral contaminations from water and CO_2 in the air.

2.2 In Situ Raman Spectroscopy

The Raman scattering light from the catalyst surfaces in each reaction channel was collected by the attached Raman probe. The Raman probe used in this study, which has been described in detail elsewhere [30], was built to work in a backward scattering mode. The excitation laser beam (514.5 nm) generated by an argon ion laser (Coherent, Innova 400) was divided into six beams; each of these beams was transmitted to a Raman probe via an optical fiber. The laser power was about 15 mW at the catalyst surface, and a typical accumulation time used in this experiment was 60 s. The six optical fibers from the Raman probes were coupled to a multi-leg fiber bundle (Princeton Instruments, 10-leg fiber bundle), which allowed one spectrometer (Princeton Instruments, Spectrapro 2500*i*) to be used for simultaneous monitoring up to 10 Raman probes. By passing the Raman lights through a long band pass filter that blocks Rayleigh scattering lights, the net Raman scattering lights were dispersed by a 600 lines/mm grating and simultaneously recorded on a charge-coupled device (Princeton Instruments, Spec 10, 1340 × 400 array), which allowed spectra to be recorded in a spectral range of 0–3100 cm^{-1}.

2.3 Catalyst Preparation

The V_2O_5/SiO_2 catalysts were obtained by impregnating the silica support with an aqueous solution of ammonium metavanadate (NH_4VO_3, Sigma-Aldrich, >99.99%) dissolved in oxalic acid ($HO_2CCO_2H \cdot 2H_2O$, Sigma-Aldrich, 99%). Various weight loadings of V_2O_5/SiO_2 were obtained by varying the concentration of vanadium

compound in the aqueous solution. The V_2O_5/SiO_2 catalysts were dried overnight at 110 °C and calcined in dry air at 550 °C for 2 h after the impregnation. Each catalyst powder was pressed against a 0.8-mm-thick, stainless-steel foam (Porvair, PPI #80) to make a sample strip; each strip carried ~80 mg net V_2O_5/SiO_2 catalyst. The silica support used in this experiment was silica gel (SiO_2, Davisil 645, #60–100, 300 m^2/g) without further treatment. The sample strips were calcined at 550 °C for 2 h in a furnace and loaded into the reactor immediately prior to the experiments. For Raman measurement at the fully dehydrated condition, the catalysts were further treated by heating in the reactor to 350 °C in situ and then holding at this temperature for 1 h to remove moisture absorbed in the process of mounting the catalysts to the reactor cell. The reactor then was cooled to 100 °C for in situ Raman measurements. Ultra high-purity (99.9999%) O_2 flowed through the reactor at a flow rate of 12 standard cubic centimeters per second (SCCM) during the entire Raman measurements under the dehydrated condition. For the *operando* measurements, a flow of He (99.9999%, 2 SCCM), which was controlled by a mass flow controller (Brooks), passed through an ice-bath-cooled methanol bubbler to carry saturated methanol vapor (4%). The CH_3OH/He gaseous mixture was further combined with an ultra-high-purity oxygen gas flow (1 SCCM), which was controlled by a second mass flow controller, and then introduced into the HTO reactor. Identical flow of six reactors was assured by using a flow register that was positioned at the entrance of the six-reaction channels [30]. The detailed data acquisition and analysis method has been described in elsewhere [30], so it will not be repeated in here.

3 Results

In situ Raman spectra of the V_2O_5/SiO_2 were measured simultaneously by six Raman probes. Detailed Raman spectra of dehydrated V_2O_5/SiO_2 catalysts with different vanadium loadings are compared in Fig. 2a. At 0% loading of V_2O_5, the Raman bands from the SiO_2 support surface are observed at 1064, 972, 802, and 604 cm^{-1}. These Raman bands for the SiO_2 support are consistent with that reported in the literature; that is, Raman bands at ~1050 (the asymmetric mode of Si–O–Si linkages), ~979 (surface silanol groups), ~452 and ~803 (siloxane linkage), 488 and ~605 cm^{-1} (three-fold siloxane ring) [31]. With increasing V_2O_5 loadings, the Raman bands of the SiO_2 support gradually lose intensity, and the Raman signatures of vanadium oxide species gain increasing intensity. The strong Raman band at 1036 cm^{-1} in Fig. 2a apparently corresponds to the vanadium-containing species because its intensity increased dramatically with the increase of vanadium loading. It has been well documented that the band at 1036 cm^{-1} is associated with the mono-oxo V = O stretch bond of isolated VO_4 units on the SiO_2 support [25]. A weak, broad band around centered at ~915 cm^{-1} is also

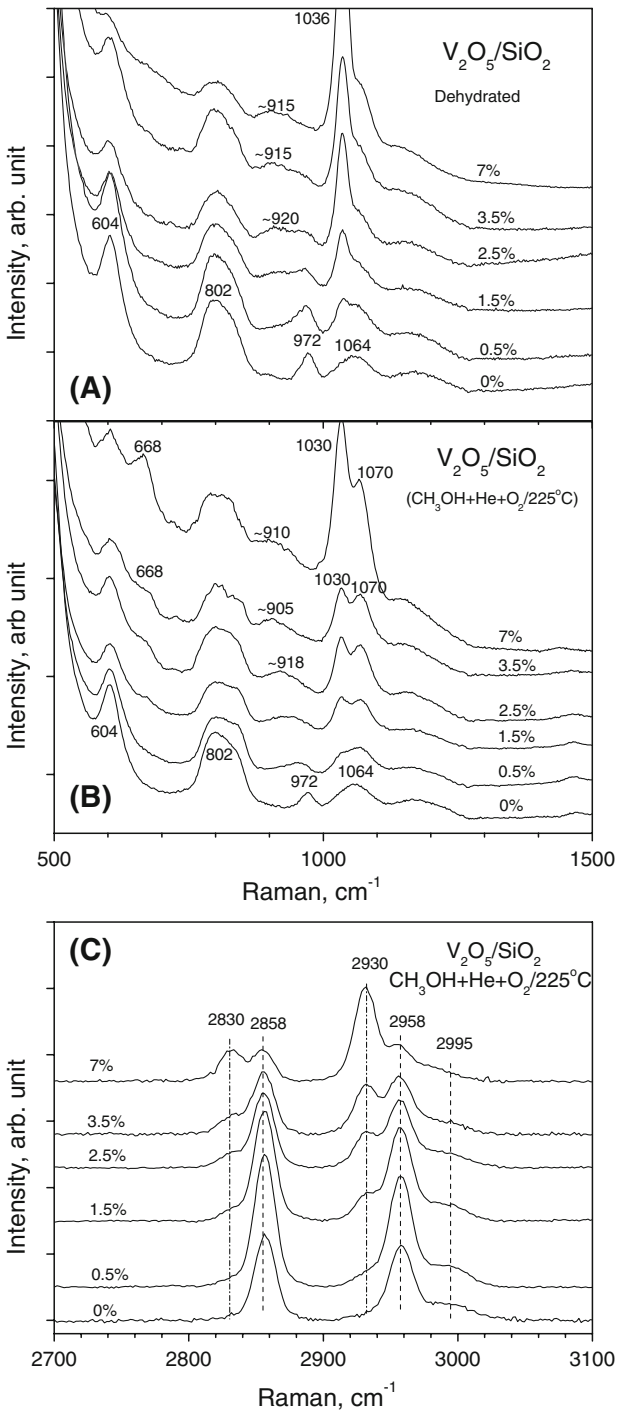

Fig. 2 In situ Raman spectra of the V_2O_5/SiO_2 catalysts at different experimental conditions. (**a**) 500–1500 cm^{-1} at the dehydrated condition. (**b**) 500–1500 cm^{-1} at 225 °C under the gaseous mixtures. (**c**) 2700–3100 cm^{-1} at 225 °C under the gaseous mixtures

from V_2O_5 because its intensity grows with increasing V_2O_5 loading.

The *operando* Raman spectra in the 500–1500 and 2700–3100 cm^{-1} regions of V_2O_5/SiO_2 catalysts with various vanadium loadings during methanol oxidation at 225 °C are shown in Fig. 2b and c, respectively. Two additional Raman bands appear at 1070 and 668 cm^{-1} in Fig. 2b as compared to spectra of the dehydrated V_2O_5/SiO_2 samples in Fig. 2a. Apparently, the two Raman bands at 1070 and 668 cm^{-1} are associated with the reaction intermediates on the V_2O_5/SiO_2 catalyst surface. In the literature, the band at 1070 and 668 cm^{-1} have been attributed to V = O and bridging V–O–CH_3 vibration, respectively [32]. In the 2700–3100 cm^{-1} region, the Raman spectrum of the pure SiO_2 support shows three bands (Fig. 2c). The intensities of the Raman bands at 2858, 2958, and 2995 cm^{-1} increase at low V_2O_5 loading and decrease at higher loading. The weak peak at 2995 cm^{-1} has been identified by IR as arising from the asymmetric C–H stretch vibrational mode of the surface methoxy group on the SiO_2 support (Si–OCH_3); the intense peaks at 2958 and 2858 cm^{-1} are from the symmetric C–H stretch vibrational mode [33]. The *operando* Raman spectra of the V_2O_5/SiO_2 catalysts during methanol oxidation in the 2700–3100 cm^{-1} region have two distinctive peaks at 2830 and 2930 cm^{-1}. The intensities of these peaks increase with increasing V_2O_5 loading. The bands at 2830 and 2930 cm^{-1} were attributed to the symmetric C–H stretch mode of surface vanadium methoxy species (V–OCH_3) on the silica support [21, 32].

The *Operando* Raman spectra of the 3.5 wt% V_2O_5/SiO_2 catalyst at various reaction conditions are shown in Fig. 3a and b for the 500–1500 and the 2700–3100 cm^{-1} regions, respectively. The Raman bands resulting from the V–OCH_3 intermediates at 664, 1070, 2830, and 2930 cm^{-1} appeared when gaseous reactant mixtures ($CH_3OH + H_2 + O_2$) were passed over the catalysts, and these bands lost intensity at high temperatures. However, the Raman band of the Si–OCH_3 species at 2858, 2958, and 2995 cm^{-1} were still observed at up to 325 °C under flowing O_2. The V = O terminal bond at 1036 cm^{-1} has a ~6 cm^{-1} shift toward the lower wave number (red-shift) side.

The IR spectra of the gaseous mixtures in the reaction channels loaded with a 3.5 wt% V_2O_5/SiO_2 catalyst at various experimental conditions are shown in Fig. 4. The background IR spectrum of the HTO reactor was recorded by flowing He and O_2 at 100 °C. To indentify IR bands belonging to CH_3OH, the IR spectrum of gaseous mixtures in the HTO reactor was taken at 100 °C, because no reaction took place on the V_2O_5/SiO_2 catalyst at 100 °C. The strong absorption bands *a*, *e*, and *f* in Fig. 4 correspond to the C–O stretch, CH_3 d- and s-stretch, and O–H stretch

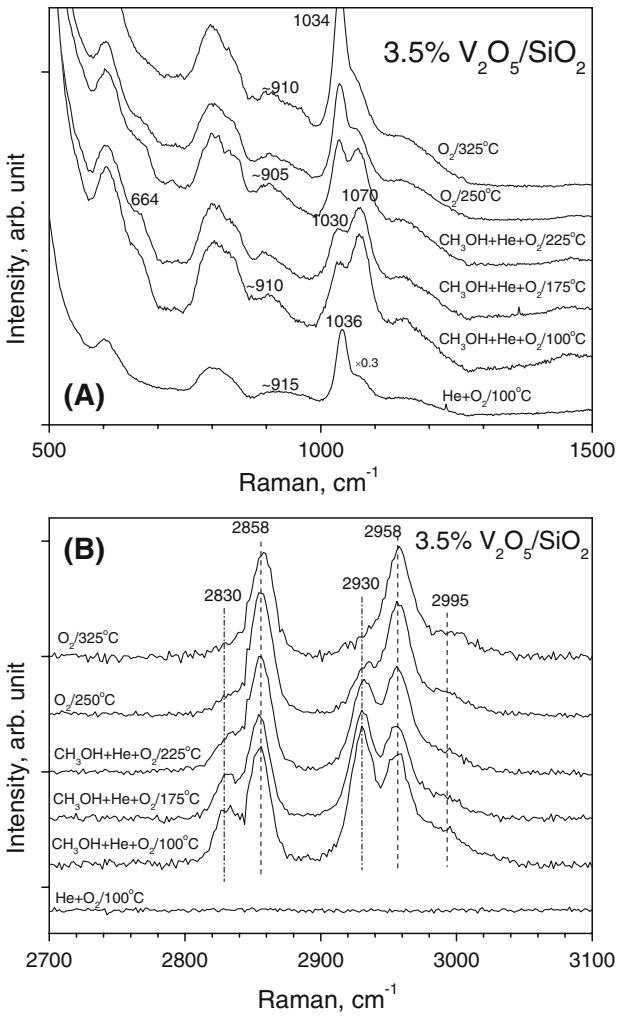

Fig. 3 In situ Raman spectra of 3.5% wt V_2O_5/SiO_2 catalyst at different reaction stages. (**a**) 500–1500 cm^{-1}. (**b**) 2700–3100 cm^{-1}

of CH_3OH, respectively. The spectrum obtained at a reactor temperature of 225 °C shows some additional strong IR absorption bands compared to the spectrum at 100 °C. The *b* band corresponds to the C–O stretch and CH_3 rock of methyl formate (MF); the *c* band arises mainly from the C–O stretch of formaldehyde (FA); and the *d* band is the characteristic band of the C–O stretch in CO_2. By integrating each band, CH_3OH conversion as well as yields for various products (e.g., FA, MF, and CO_2) can be calculated from the methanol partial oxidation reaction on the V_2O_5/SiO_2 catalyst [34].

Figure 5 shows CH_3OH conversion and the relative intensities of the IR bands assigned to the products as a function of the reaction temperatures. The low CH_3OH conversion detected at 100 and 150 °C suggests that the reaction activities are low in this temperature range. With increasing reaction temperature, the CH_3OH conversion increased. Product selectivity cannot be directly obtained from the intensity plots because the IR bands have different

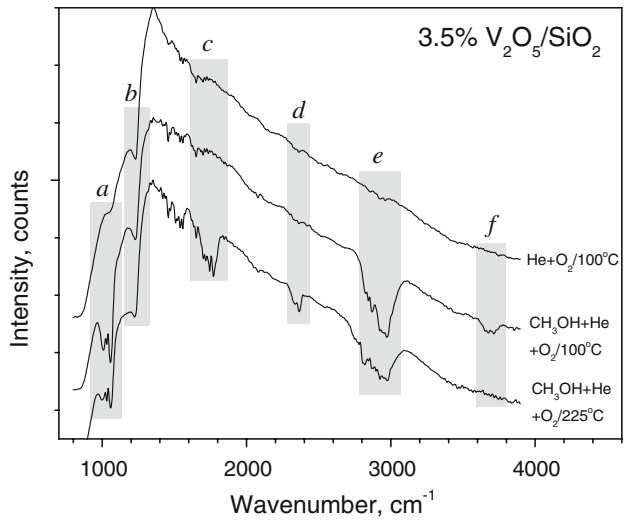

Fig. 4 FT-IR spectra of the reaction channel loaded with 3.5% wt V_2O_5/SiO_2 catalyst. The spectra were displayed with offsets. *a*: C–O str. of CH_3OH, *b*: C–O str. and CH_3 rock of MF, *c*: C–O str. of FA, *d*: C–O str. of CO_2, *e*: CH_3 and CH_2 d- and s-str. of CH_3OH, FA, and MF, *f*: O–H str. of CH_3OH

IR absorption coefficients. However, the CH_3OH conversion (Fig. 5a) and the FA intensity plots (Fig. 5c) show a very similar trend as a function of vanadium loadings and reaction temperatures. This is consistent with the literature in that FA is the main product from the methanol oxidation reaction on V_2O_5/SiO_2 catalysts [7, 29]. The CO_2 produced from CH_3OH oxidation is considerably lower than FA over all the V_2O_5/SiO_2 catalysts. Even though more CO_2 is produced over a pure SiO_2 support than over a supported V_2O_5 catalyst, the intensity of the CO_2 signal from the pure SiO_2 is rather low because of the low CH_3OH conversion.

4 Discussion

As shown in Fig. 2, we were able to detect and follow this critical $\sim$915-cm^{-1} band of the V_2O_5/SiO_2 catalyst under various reaction conditions (e.g., He + O_2/225 °C and CH_3OH + He + O_2/225 °C) with the *operando* Raman spectroscopy. As noted in the Sect. 3, the SiO_2 support has Raman bands at $\sim$1064, $\sim$972, $\sim$802, and $\sim$604 cm^{-1} that do not overlap with the band at $\sim$915 cm^{-1}. Although the $\sim$915-cm^{-1} band has a relatively small intensity, the signals are sufficiently strong to be quantified at various vanadium loadings, as is shown in Fig. 6. An important observation is that the band intensity at $\sim$915 cm^{-1} increases with increasing vanadium loading, whether during methanol oxidation or in the absence of methanol. This is clear evidence to support that the 915 cm^{-1} band is associated with the V_2O_5 species on the SiO_2 support. Another important observation is that the 915 cm^{-1} band did not disappear under the reaction conditions. Recently, Launay et al. reported a band at $\sim$905 cm^{-1} for V_2O_5 supported on mesoporous silica (MCM41) under air and at 600 °C [35]. They pointed out that the $\sim$905 cm^{-1} band observed in their experiment should not be assigned to peroxo species [19, 36], which is not expected to be stable at such a high temperature. Our results further confirm the assignment in the literature, where $\sim$915 cm^{-1} has been assigned as V–O–Si band [37].

Because V–OCH_3 and Si–OCH_3 are important surface intermediates in methanol oxidation over V_2O_5/SiO_2 catalysts, we integrated the intensities of the C–H stretch modes of –OCH_3 as measured at various vanadium loadings and at different reaction temperatures. Deviation in such measurement resulting from microscopic heterogeneity associated with V_2O_5 dispersion on the silica surface is expected to be insignificant because the laser beam covers an area of about 40,000 μm^2, which is more than 10 orders of magnitude larger than the area covered by a dispersed vanadium atom at half monolayer coverage. The quantitative intensity analysis of the Raman bands was performed by calibrating all six Raman probes using a TiO_2 pellet as a standard sample. Using a SiO_2 internal standard gave the same results[1]. The results of these analyses are shown in Fig. 7. An important observation not reported previously is that the intensity of Si–OCH_3 passes through a maximum as the vanadium loading increases. One might postulate that as the surface coverage of V_2O_5 increases, the Si–OCH_3 surface density on the SiO_2 support would drop, in an opposite trend to the V–OCH_3 band intensity. Hence, the intensity of Si–OCH_3 would be highest at zero vanadium loading and decreases as the vanadium loading increases. However, from our experiments, which were repeated five times, the intensity of Si–OCH_3 showed a significant increase (enhanced intensity) at low surface vanadium coverage (e.g., 0.5 and 1.5 wt%) and then started to decrease gradually as the vanadium surface coverage was increased further. The intensity of Si–OCH_3 with a vanadium loading at 2.5 wt% ($\sim$35% calculated vanadium surface coverage) is at nearly the same level when compared to the intensity at zero vanadium loading. We attribute this phenomenon to *surface cluster-edge activation*. The schematic drawing shown in Fig. 8 illustrates the *surface cluster-edge activation*. At low vanadium loadings, the V_2O_5 is highly dispersed, and it is reasonable to describe the supported vanadium oxide as isolated units. While a CH_3OH molecule is chemisorbed onto the surface of the VO_4 species to form a V–OCH_3 by

[1] The silica support band at $\sim$800 cm^{-1} can be used as an internal standard to give an relative intensity calibration for the Raman bands. Same results were obtained by internal standard silica band verse TiO2 Raman bands for calibrating Raman probes

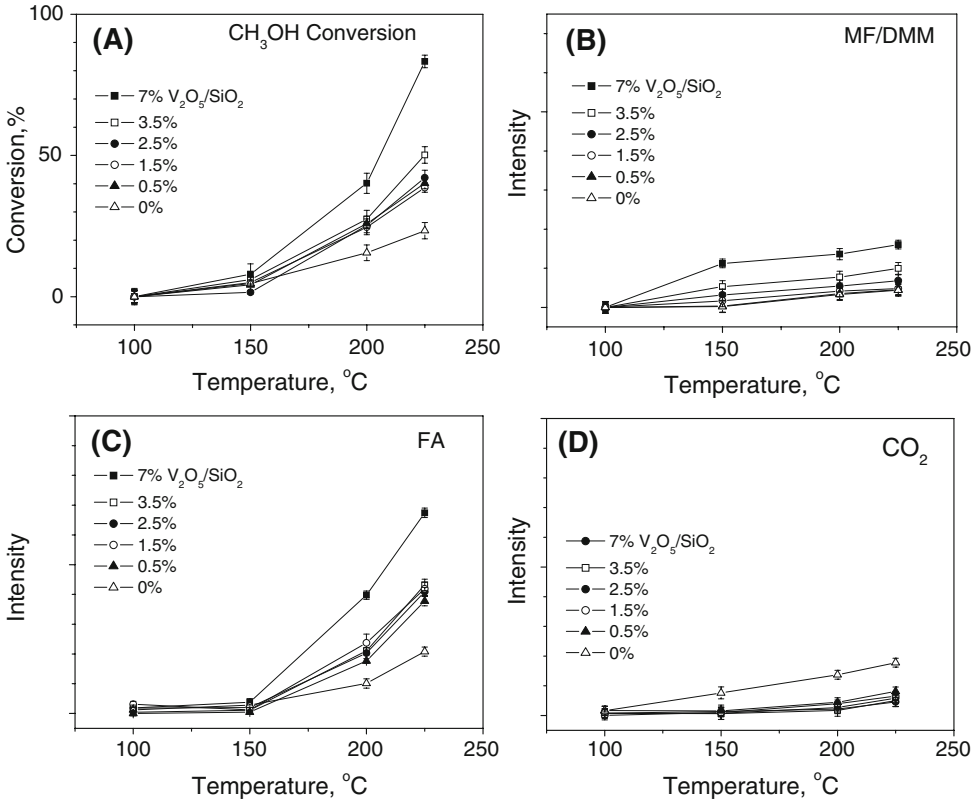

Fig. 5 The product analysis results from the FT-IR spectra. Error bars, which are the first order standard deviation, were obtained from multiple measurements

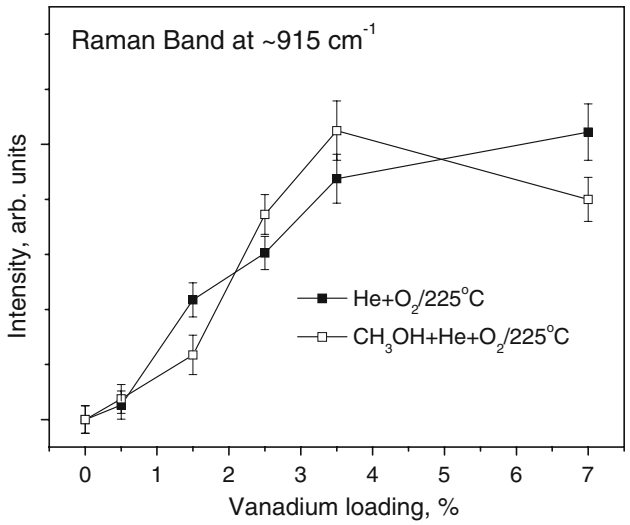

Fig. 6 Intensity of ~ 915 cm^{-1} band vs. vanadium loading under He + O_2/225 °C and CH_3OH + He + O_2/225 °C

process [1] or process [2], as shown in Fig. 8, additional Si–OH sites are produced on the surface of the SiO_2 support via process [3] and [4]. This mechanism also prevails at the edge of vanadium oxide clusters. Si–OCH_3 species formed on these new sites are observed as the enhanced Raman signal of Si–OCH_3 for the catalysts with low vanadium loadings. For the V_2O_5/SiO_2 catalyst with further increasing vanadium loading, a continuous increase in V_2O_5 cluster size is conceivable via V–O–V bonding. Hence, the fraction of vanadium oxide at edge is reduced. Therefore, the *surface cluster-edge activation* becomes less pronounced for the catalysts with high vanadium loadings as compared to those with low vanadium loadings. The ensemble surface of V_2O_5 clusters at high vanadium loadings is expected to dominate.

The intensity of V–O–CH_3 shows a different trend as a function of the reaction temperature (Fig. 7b). For reaction at or below 175 °C, a maximum V–O–CH_3 intensity is reached at 3.5% V loading. For reaction above 200 and 250 °C, the intensity continues to increase; no maximum is observed. The results indicate that more than one mechanism (active site) may be at play for V–O–CH_3 formation at different reaction temperatures. The Raman intensity of the V–O–CH_3 at a plateau for the reaction temperature at 175 °C is lower than that for the reaction at 100 °C. This decreased intensity is attributed to oxidative hydrogen cleavage at the higher temperature because the reaction did not take place at 100 °C. The results also suggest that the reaction rate determining step is not activated chemisorption of methanol [9].

A hypothesis of possible reaction mechanisms for different reaction temperatures, as shown in Fig. 9, explains the new experimental observations obtained with the *operando* reactor. At lower temperatures, most of the

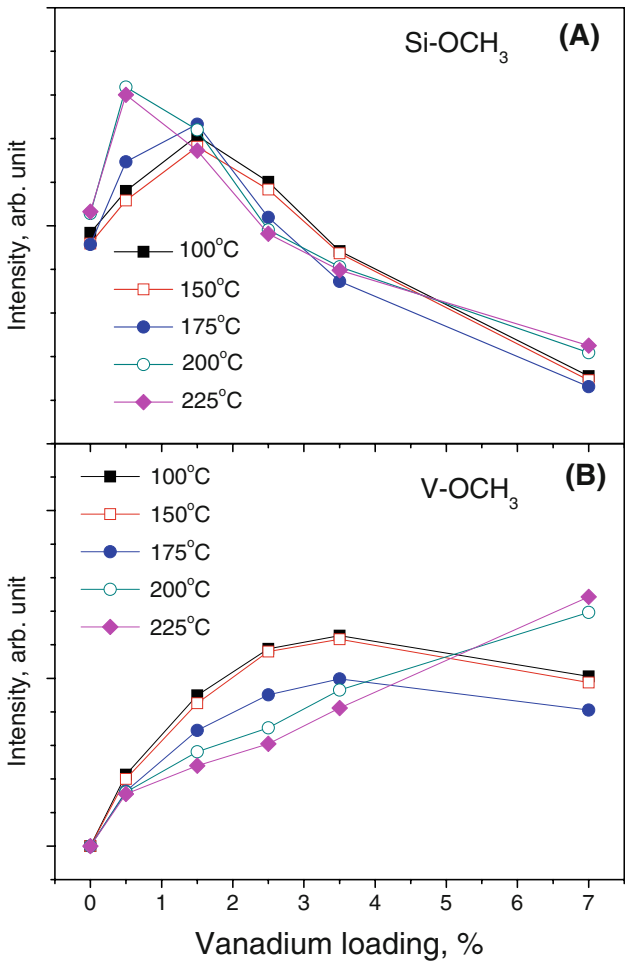

Fig. 7 Intensities of C–H stretch Raman bands (**a**) Si–OCH_3 and (**b**) V–OCH_3 with increasing vanadium loadings under different reaction temperatures

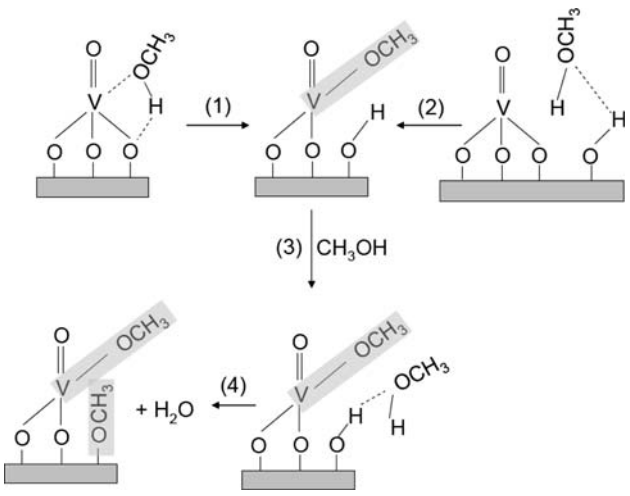

Fig. 8 Schematic drawing of the methoxy intermediates on isolated vanadium oxide species (e.g., a VO_4 unit and the SiO_2 support)

V–O–CH_3 forms at the boundary of isolated vanadium oxide species, which can be a single VO_4 site or polymeric species. Along with this process, additional Si–OH sites are produced on the surface of the SiO_2 support, which leads to additional Si–OCH_3 formation on the SiO_2 support. This also is consistent with our observation of *surface cluster edge activation*, which was described above. It is also important to note that the V–O–CH_3 intensity reaches a plateau at a half monolayer of V_2O_5 coverage at 3.5% vanadium loading for a reaction lower than 175 °C, while the Si–O–CH_3 intensity continues its further decline. Again, edge activation of methanol can be used to rationalize these remarkably unsynchronized trends between Si–O–CH_3 and V–O–CH_3 in relation to the higher vanadium loading between a half monolayer and single monolayer at lower reaction temperatures (<175 °C). As the vanadium loading increases, the silica surface area covered by the vanadium surface cluster increases and results in a continued decrease of Si–O–CH_3. However, the edge of the V_2O_5 islands appeared not to be decreased much because of specific surface cluster layer growth mechanisms. Highly dispersed V_2O_5 clusters prepared in the presence of water on a model SiO_2 surface show clear clusters and edge boundaries when observed by scanning tunneling microscopy [38].

The high selectivity of the V_2O_5/SiO_2 catalyst for FA is evident from the significantly reduced CO_2 intensity, even with a V_2O_5 loading as low as 0.5 wt%. It should be emphasized that the CO_2 signal intensity is rather low in comparison to that of the FA signal because CH_3OH activation at the cluster edge prevails.

At a higher reaction temperature above 200 °C, the Raman intensity of the C–H bond associated with V–O–CH_3 continues its ascending trend with increasing V_2O_5 loadings (Fig. 7). In accordance with the Raman results, methanol conversion (Fig. 5a) and FA intensity (Fig. 5c) increase also. The yields are very low to FM, and do not show a significant increase when the reaction temperature was increased, as shown in Fig. 5b. MF/DMM are not the main products of methanol partial oxidation on the V_2O_5/SiO_2 catalysts, and the mechanism of FA formation is therefore the mainly focus of this manuscript. For the higher reaction temperatures (>200 °C), both the VO_4 sites at the edges and the surfaces of the V_2O_5 clusters are active as is suggested by the continuous increases of V–O–CH_3 Raman band intensities as a function of vanadium loadings. As shown in Fig. 9, we propose that the surface of the V_2O_5 cluster also becomes active to form V–O–CH_3, which is consistent with the increased V–OCH_3 Raman signals and the dramatically increased reaction activities at higher temperatures.

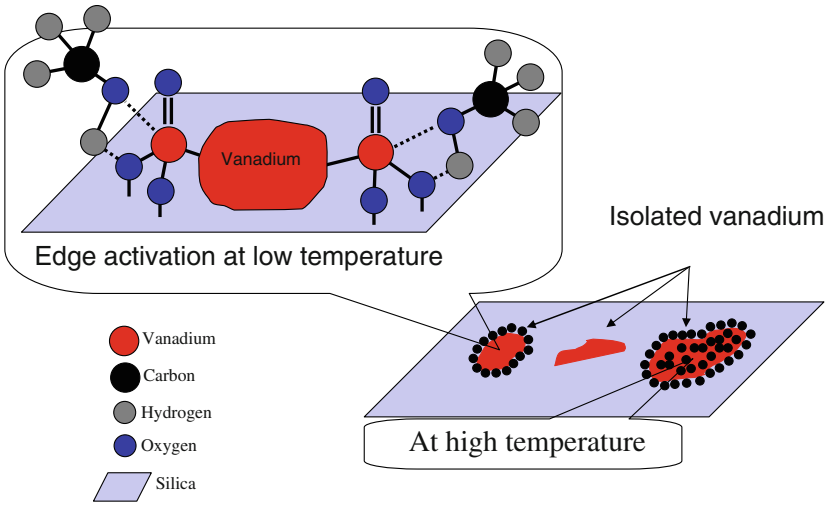

Fig. 9 Schematic illustration of *surface cluster-edge activation* mechanism related to a low reaction temperature regime. The mechanism for a high reaction temperature regime is also shown

5 Conclusions

In this study, we used an HTO reactor to study V_2O_5/SiO_2 catalysts with different vanadium loadings. Integration of FT-IR imaging for product analysis coupled with in situ Raman spectroscopic catalyst characterization enabled us to obtain a novel insight into the reaction mechanism of methanol partial oxidation over V_2O_5/SiO_2 catalysts, especially for the V–O–CH_3 formation on VO_4 sites, as well as for Si–O–CH_3 formation on SiO_2 supports. Monitoring Si–O–CH_3 as a function of vanadium loadings (Fig. 7a) by *operando* Raman spectroscopy suggests that an *edge activation mechanism* may play an important role for formation of Si–O–CH_3 on SiO_2 supports. Two different trends of V–O–CH_3 band intensity with increasing vanadium loadings are observed in different reaction temperature regimes (Fig. 7b), suggest that V–O–CH_3 was most likely formed at VO_4 located at the edge of V_2O_5 surface clusters at low reaction temperatures (<175 °C). At higher reaction temperatures, V–O–CH_3 appeared to be formed on the surfaces of whole clusters as well as on edge sites. By monitoring the occurrence and variation of the ~915-cm^{-1} Raman band of vanadium species on the SiO_2 support under real reaction conditions we concluded that this band is not involved in the methanol oxidation reaction.

Acknowledgments This work was supported by Pacific Northwest National Laboratory (PNNL) under the Laboratory Directed Research and Development project entitled Combinatorial Operando Catalysis Research. The authors also wish to acknowledge the Institute for Interfacial Catalysis and the W.R. Wiley Environmental Molecular Science Laboratory, a national scientific user facility located at PNNL.

References

1. Wilson SR, Czarnik AW (1997) Combinatorial chemistry: synthesis and application. Wiley, New York
2. Gordon EM, Kerwin JF (1998) Combinatorial chemistry and molecular diversity in drug discovery. Wiley, New York
3. Topsoe H (2003) J Catal 216:155
4. Wainwright MS, Foster NR (1979) Catal Rev 19:211
5. Bosch H, Janssen F (1988) Catalysis Today 2:369
6. Bond GC, Tahir SF (1991) Appl Catal 71:1
7. Deo G, Wachs IE (1994) J Catal 146:323
8. Briand L, Gambaro L, Thomas H (1996) J Catal 161:839
9. Busca G (1996) Catalysis Today 27:457
10. Burcham LJ, Wachs IE (1999) Catalysis Today 49:467
11. Tatibouet JM (1997) Appl Catal A Gen 148:213
12. Weckhuysen BM, Keller DE (2003) Catalysis Today 78:25
13. Oyama ST, Went GT, Lewis KB, Bell AT, Somorjai GA (1989) J Phys Chem 93:6786
14. Went GT, Oyama ST, Bell AT (1990) J Phys Chem 94:4240
15. Khodakov A, Olthof B, Bell AT, Iglesia E (1999) J Catal 181:205
16. Burcham LJ, Deo GT, Gao XT, Wachs IE (2000) Top Catal 11:85
17. Bronkema JL, Bell AT (2007) J Phys Chem C 111:420
18. Tanaka T, Yamashita H, Tsuchitani R, Funabiki T, Yoshida S (1988) J Chem Soc Farad Trans I 84:2987
19. Keller DE, de Groot FMF, Koningsberger DC, Weekhuysen BM (2005) J Phys Chem B 109:10223
20. Busca G (1988) Mater Chem Phys 19:157
21. Burcham LJ, Badlani M, Wachs IE (2001) J Catal 203:104
22. Eckert H, Wachs IE (1989) J Phys Chem 93:6796
23. Yoshida S, Tanaka T, Hanada T, Hiraiwa T, Kanai H, Funabiki T (1992) Catal Lett 12:277
24. Wachs IE, Weckhuysen BM (1997) Appl Catal A Gen 157:67
25. Hardcastle FD, Wachs IE (1991) J Phys Chem 95:5031
26. van Lingen JNJ, Gijzernan OLJ, Weckhuysen BM, van Lenthe JH (2006) J Catal 239:34
27. Wachs IE (1996) Catalysis Today 27:437
28. Weckhuysen BM, Jehng JM, Wachs IE (2000) J Phys Chem B 104:7382
29. Khaliullin RZ, Bell AT (2002) J Phys Chem B 106:7832

30. Li G, Hu D, Xia G, White JM, Zhang C (2008) Rev Sci Instrum 79:74101
31. Jehng JM, Wachs IE (1992) Catal Lett 13:9
32. Jehng JM, Hu HC, Gao XT, Wachs IE (1996) Catalysis Today 28:335
33. Kim DS, Ostromecki M, Wachs IE (1995) Catal Lett 33:209
34. National Institute of Standard and Technology (NIST) Chemistry Webbook (2005) http://www.webbook.nist.gov/chemistry/
35. Launay H, Loridant S, Pigamo A, Dubois JL, Millet JMM (2007) J Catal 246:390
36. Magg N, Immaraporn B, Giorgi JB, Schroeder T, Baumer M, Dobler J, Wu ZL, Kondratenko E, Cherian M, Baerns M, Stair PC, Sauer J, Freund HJ (2004) J Catal 226:88
37. Lee EL, Wachs IE (2007) J Phys Chem C 111:14410
38. Kaya S, Sun YN, Weissenrieder J, Stacchiola D, Shaikhutdinov S, Freund HJ (2007) J Phys Chem C 111:5337